



Article

Layout Optimization of a Tidal Current Turbine Array Based on Quantum Discrete Particle Swarm Algorithm

Yanan Wu ¹, He Wu ^{1,*}, Hooi-Siang Kang ²  and He Li ³ 

¹ National Ocean Technology Center, 219 Jieyuanxi Road, Nankai District, Tianjin 300112, China; hdwuyan@163.com

² Marine Technology Center, Institute for Vehicle Systems and Engineering, University Teknologi Malaysia, Johor Bahru 81310, Malaysia

³ Centre for Marine Technology and Ocean Engineering (CENTEC), Instituto Superior Técnico, Universidade de Lisboa, 1049-001 Lisbon, Portugal

* Correspondence: wh_crane@163.com; Tel.: +86-15822728335

Abstract: This article focuses on the optimization of the layout of a tidal current turbine array (TCTA) using the Quantum Discrete Particle Swarm (QDPS) algorithm. The objective of the optimization is to balance the maximum energy output and minimum levelized cost of energy (LCOE). The optimization model proposed in this paper was constructed by combining a computational tidal model and the QDPS algorithm, which incorporate several advancements, including modeling of underwater terrain, obtaining tidal current field using high-fidelity ocean model, considering turbine properties, formulating partial influence of wakes on turbines, accounting for interactions between multiple wakes, modeling of safe operating distance, developing an LCOE model, and computing the sea space utilization area of a tidal farm. The proposed method was applied to optimize the layout of TCTA in a real waterway, which employed maximum tidal current fields during flooding and ebbing periods of spring tides as input for safety reasons. The results indicate that compared to a regular staggered layout, the total power generation improved by 19% and 16%, and the LCOE reduced by 12% and 15%, respectively, when the concluded optimized layout was utilized. Sea area decreased by 24% when LCOE was minimum. Overall, the proposed method has a better performance and can support the set selection as well as turbines placements of tidal current farms.



Citation: Wu, Y.; Wu, H.; Kang, H.-S.; Li, H. Layout Optimization of a Tidal Current Turbine Array Based on Quantum Discrete Particle Swarm Algorithm. *J. Mar. Sci. Eng.* **2023**, *11*, 1994. <https://doi.org/10.3390/jmse11101994>

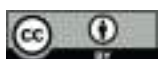
Academic Editor: Atila Incecik

Received: 6 September 2023

Revised: 29 September 2023

Accepted: 3 October 2023

Published: 16 October 2023



Copyright: © 2023 by the authors. Licensee MDPI, Basel, Switzerland. This article is an open access article distributed under the terms and conditions of the Creative Commons Attribution (CC BY) license (<https://creativecommons.org/licenses/by/4.0/>).

Keywords: tidal energy; tidal current turbine array; quantum discrete particle swarm; levelized cost of energy

1. Introduction

Oceanic tides have the potential to be used for yielding vast amounts of power. Tidal current turbines are one of the important technologies employed to harness the kinetic energy of tides [1,2]. To maximize extractable energy, multiple turbines will need to be deployed in an array [3]. Therefore, reliability and stability of tidal turbines are very important and should be continually improved in-line with rapid commercialization progress for tidal current energy. Recently, an increasing number of successful tidal current projects have emerged, such as the MeyGen project in the UK [4] and the LHD tidal power demonstration site in China [5]. Generally, a tidal farm is deployed with equal spacing of the tidal current turbine array (TCTA), similar to the empirical layout of a wind farm [6,7]. However, the positioning and individual tuning of each turbine could have a substantial impact on the global power generation due to the wake influence behind turbines and other factors [8–10]. Moreover, the wake of individual turbines interacts with each other, and the hydrodynamic structure is quite complex, which is considered as the main influence on array performance [11]. Thus, study on layout optimization of TCTA is a critical consideration in large-scale exploitation of tidal current energy, which

concerns the utilization efficiency of generating devices and the economic benefit of the tidal power station [12].

The layout optimization of TCTA has been addressed in several earlier studies using various optimization algorithms, wake models and numerical techniques, and certain improvements in power performance have been achieved. There are three different approaches to reduce the detrimental effect of wake in a tidal farm: using flume experiments to analyze the wake interaction between turbines placed in an array, parameterization of the tidal current turbines using computational fluid dynamics (CFD), and the use of intelligent algorithms in combination with an analytical wake model.

The first approach determines the optimum array layout using scaled flume experiments or numerical flume simulations. For scaled experiments with real flow conditions of the Alderney Race [11,13], Myers and Bahaj [7] suggested a longitudinal spacing of 15 turbine diameters and a lateral spacing of 3 diameters. Mycek et al. [14,15] also used flume experiments to analyze the wake effect between turbines placed in an array. Stallard et al. [16] experimentally investigated the mean wake of a three-bladed horizontal-axis tidal stream turbine operating in a wide flume. Nash et al. [17] developed a multiscale nested model to simulate the effects of turbine and energy yields of tidal turbines. Their results indicated that a staggered array was preferred compared to a regularly spaced array. Lee et al. [18] used a three-dimensional numerical flume model to investigate how the distance between adjacent rows in a traditional crossing layout impacts the efficiency of turbines. Their findings showed that the appropriate distance between adjacent rows of turbines was approximately three times the turbine diameter. Divett et al. [19] compared the power production of four different layouts in a rectangular numerical channel and found that the power could be improved by over 50% compared to a regular layout. Additionally, multilayer perceptron neural network (MLP-NN) also was introduced to establish the interrelation between the incoming flow conditions and the wake profiles [20]. It should be noted that these studies highlighted the flow interactions between turbines placed in an array and depicted the fine-scale wake characteristics. However, only certain idealized bathymetry was simulated, which means the results are hardly to be utilized directly because various real conditions were not considered, such as realistic terrain and complex flow fields.

The second approach uses complex ocean models for accurate prediction of the hydrodynamic conditions, wake of the turbines, and power production. The available tidal energy resource could be assessed using such models. The representation of turbines in these models is typically accomplished using the blade element momentum (BEM) theory, with the actuator disk, immersed body force turbine, or frozen rotor methods used to simulate the wake deficit. Roc et al. [21,22] extended the actuator disk concept to three-dimensional large-scale ocean circulation models by adapting both the momentum and turbulence transport equations of Regional Ocean Model System (ROMS). They developed an assessment tool framework for optimizing the layout of a tidal current turbine array. Gebreslassie et al. [23] investigated the influence of wake interaction in a staggered configuration using the CFD-based immersed body force turbine modeling method. To consider the rotation effect, the detailed geometry of ocean current generators was included in the computational domain by Lee et al. [18] using the frozen rotor method. Malki et al. [24] conducted simulations of groups of tidal stream turbines using a coupled BEM-CFD model. Their results indicated that the total power production of the array could be increased by over 10% in comparison with a regular staggered layout. Stansby and Stallard [25] used the velocity deficit superposition approach to move the initial positions of the turbines using an algorithm based on the chain rule. The above studies have demonstrated the potential for improving performance by changing turbine positions. However, manual optimization of the turbine positions based on simulated results becomes difficult when hundreds of turbines are placed in a tidal farm. A notable exception is the work by Funke et al. [26–28], who optimized a TCTA layout by combining a flow model, described with partial differential equations, using a gradient optimization algorithm. Their method suggested that

power production could be increased by 33% in comparison with the classically aligned configuration. Moreover, their approach combined realistic bathymetry, flow fields, and automatic optimization. And this model developed by Funke et al. [26] was already used for the investigation of array layout of tidal stream turbines on energy extraction efficiency by Zhang et al. [29].

The third approach uses intelligent optimization algorithms, such as genetic algorithm, ant colony algorithm, and firefly algorithm, to resolve the optimization problem. In wind farm studies, some popular optimization algorithms are the genetic algorithm [28,30,31] and the particle swarm optimization (PSO) algorithm. The PSO algorithm is generally preferred over the genetic algorithm because it converges faster and provides comparatively better results, as demonstrated by Pookpant and Ongsakul [32]. Wang et al. [33] proposed a micro-siting method based on a differential evolution algorithm for the *Guishan* waterway in China. Liu et al. [34] proposed an improved PSO algorithm based on an adaptive penalty function to optimize the wake flow, water depth, and cost considerations. Wu et al. [35] proposed an optimization method based on a discrete PSO algorithm, which resulted in a 6.19% increase compared to an empirical staggered configuration. Lo Brutto et al. [36] used a semi-analytical method to optimize the arrangement of tidal turbines with a small diameter-to-depth ratio. They employed a PSO algorithm coupled with an analytical wake model [37] to represent the interaction between the turbines' wakes.

In summary, previous research has made some progress in CFD or ocean simulation, analytical wake model and optimization algorithm. However, some key factors still are not taken into account, such as underwater terrain, LCOE model, and the sea space utilization area of a tidal farm. This study firstly proposes a QDPS algorithm to resolve the multi-parameter and multi-constraint problem of layout optimization. The main objective is to increase power production and decrease levelized cost of energy (LCOE), with tidal current speed and turbine diameter as controlling parameters. Additionally, safe operating distance and water depth were considered as auxiliary constraints. The problem was formulated as the optimal layout that maximizes energy generation or minimizes LCOE. Finally, the proposed framework for layout optimization of TCTA was verified using tidal current data from the *Putuo-Hulu* waterway in the *Zhoushan* Islands, China. The novel contribution of this paper includes the following: constructing the optimization framework of TCTA layout, proposing an optimization algorithm of TCTA layout based on QDPS, considering six main factors and constraints, and regarding LCOE as an important objective.

The rest of the paper is arranged as follows: Section 2 discusses the optimization framework, Section 3 explains the QDPS algorithm, Section 4 validates the optimization framework, the results are listed in Sections 5 and 6 provides the conclusions.

2. The Optimization Framework

The optimization model proposed in this paper incorporates several advancements, including modeling of underwater terrain, obtaining tidal current field using high-fidelity ocean model, considering turbine properties (such as diameter and conversion efficiency), formulating partial influence of wakes on turbines, accounting for interactions between multiple wakes, modeling of safe operating distance, developing an LCOE model, and computing the sea space utilization area of a tidal farm.

The optimization algorithm framework, as shown in Figure 1, consists of six sections: underwater terrain and tidal model, analytical wake model, wake merging schemes, safe distance constraint, sea space utilization model, and cost model. This section provides a description of the methodology employed in the proposed optimization model.

2.1. Underwater Terrain and Tidal Model

Accurate modeling of the hydrodynamic characteristics of tidal flow is essential to optimize the layout of a tidal farm. In this paper, a high-fidelity computational ocean model was constructed for the area of case study based on the finite volume community ocean model (FVCOM) [38] using unstructured triangular meshes. The distribution of

kinetic energy of tidal current in this area was analyzed to estimate the potential amount of tidal energy. A detailed description of the computational domain and the validation are presented in Section 4.

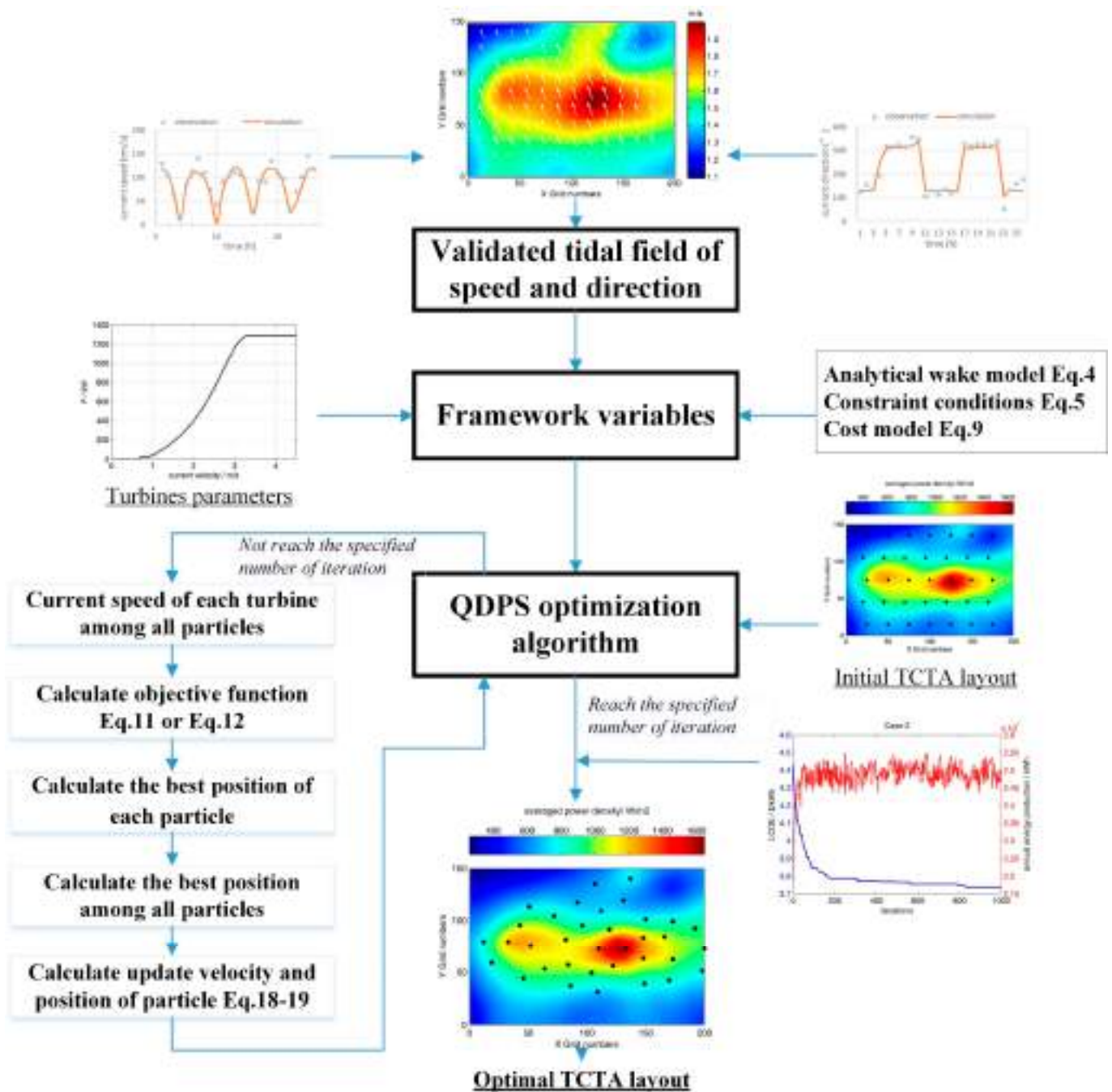


Figure 1. Framework of the proposed TCTA layout optimization process.

2.2. Analytical Wake Model

Tidal turbine wakes have a strong impact on tidal farms as they affect the power output and the turbulence level. An analytical wake model is used to describe the downstream flow field of turbines, which is achieved based on theoretical derivation or experiment. Several wake models, including the Lissaman, Ainslie, Jensen, and Larsen models, have been applied to address the issue of micro-siting in wind farms. And some research results [15,16,39–41] have been presented on tidal turbine wake flow.

In this paper, Jensen’s model [42] was adopted due to its simplicity of calculation; it is also a wind analytical wake model. The main features in this model are that the wake expands linearly with downstream distance, and the velocity deficit has a top-hat shape in the wake regions. Previous studies [36,37,39] show the applicability of Jensen’s model to tidal applications. The structure of the wake model is illustrated in Figure 2, where u_j is the incident velocity at tidal turbine j , D is the turbine blade diameter, and $u_{i,j}$ and $D_{i,j}$ are the velocity and diameter, respectively. The wake spreads to turbine i , and x is the distance between turbines i and j . $z_j = [x_j, y_j, z_j]$ and $z_i = [x_i, y_i, z_i]$ represent the positions of turbines in directions of i and j , respectively. When the condition in Equation (1) has been satisfied, the turbine i is influenced by the wake flow of turbine j .

$$\sqrt{(y_i - y_j)^2 + (h_i - h_j)^2} < \frac{D_{i,j}}{2} \tag{1}$$

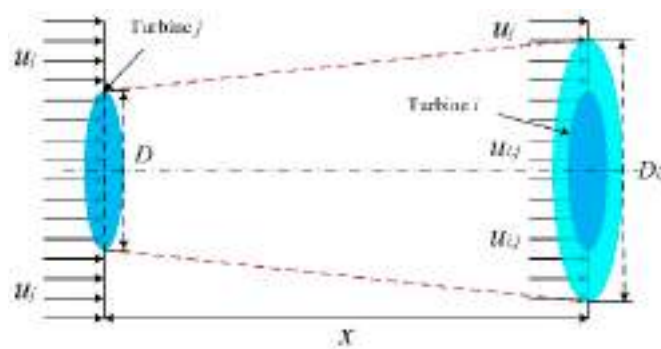


Figure 2. Structure of turbine wake flow.

If the boundary of the wake flow expands linearly, it can be described as

$$D_{i,j} = 2\alpha x + D \tag{2}$$

where α is the attenuation constant of the wake flow; typical value is 0.1. The incident velocity at turbine i is described as follows:

$$u_{i,j}(z_i, t) = u_j(z_j, t) \left[1 - \left(1 - \sqrt{1 - C_T} \right) \left(\frac{D}{D_{i,j}} \right)^2 \right] \tag{3}$$

where $u_{i,j}(z_i, t)$ and $u_j(z_j, t)$ are the positions in the coordinate system of $u_{i,j}$ and u_j , respectively, and C_T is the turbine thrust coefficient.

2.3. Wake Merging Schemes

In a TCTA, each turbine could be affected by the wake flow of the other turbines. A typical structure of a multiple wake model is illustrated in Figure 3, where turbine i is in the wake flow of both turbine j and turbine k .

Based on the law of energy conservation, the incident velocity of turbine i in a multiple wake flow can be calculated as follows:

$$u_i(z_i, t) = u_0(t) - \sqrt{\sum_{j=1, j \neq i}^{N_t} \phi_j (u_j(z_j, t) - u_{i,j}(z_i, t))^2} \tag{4}$$

where N_t is the number of tidal turbines, $u_0(t)$ is the initial flow velocity without tidal turbines, and ϕ_j depends on the relative locations of the tidal turbines. If the relative locations satisfy Equation (1), then $\phi_j = 1$; otherwise, $\phi_j = 0$.

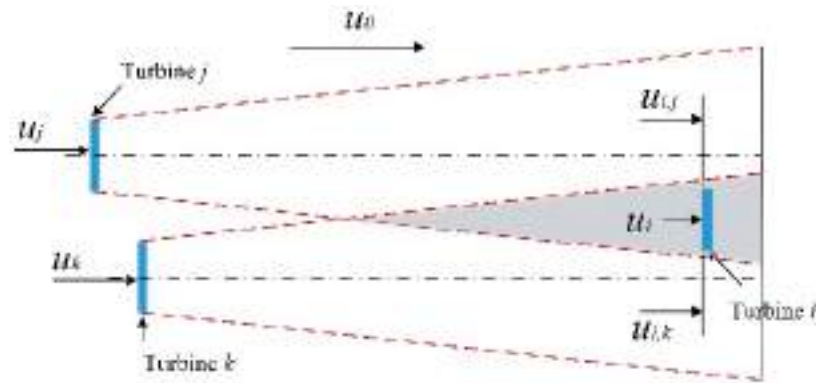


Figure 3. Structure of a multiple wake model.

2.4. Safe Distance Constraint

The safe distance is the minimum distance between any two turbines that allows for safe operation, as expressed in Equation (5). In this paper, the rounded model of safe distance was chosen, in which the same transverse and longitudinal safe distances are set as

$$d_{i,j} = 1 - \sqrt{\frac{(x_i - x_j)^2}{d_x^2} + \frac{(y_i - y_j)^2}{d_y^2} + \frac{(h_i - h_j)^2}{d_z^2}} \quad (5)$$

where $d_{i,j}$ is the constraint of the position, and d_x , d_y , and d_z are the safe distances in the transverse, longitudinal, and vertical directions, respectively. If $d_{i,j} < 0$, the constraint of safe distance is met; otherwise, it is not the safe distance.

2.5. Sea Space Utilization Model

In addition to power generation, the topographic condition is another important aspect that is considered to design the layout of a tidal current farm. It can be quantified in terms of research sea area, shape, and orientation. The sea space utilization model in the layout optimization framework can be used to quantify the area used by the tidal current farm. The boundary of the tidal current farm can be approximated by computing a convex hull in two dimensions, where the convex hull of a set is the smallest convex polygon that contains all the points, as shown in Figure 4. The convex hull was computed using Graham’s scan algorithm [43]. The area of the polygon was computed using the shoelace formula [44], shown as Equation (6), where x_i and y_i are the x and y coordinates, respectively, of point i , and n is the total number of points included in the convex hull.

$$A = \frac{1}{2} \sum_{i=0}^{n-1} (x_i y_{i+1} - x_{i+1} y_i) \quad (6)$$

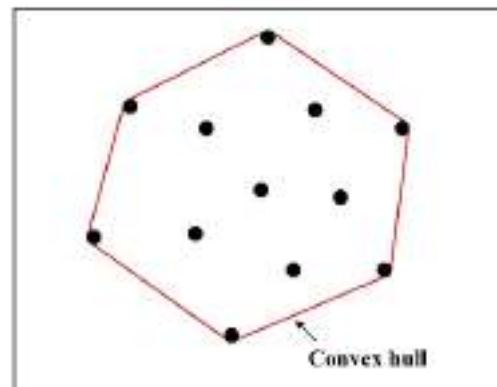


Figure 4. Convex hull (red) of a set of scattered points (black) representing tidal turbines in two dimensions.

2.6. Cost Model

LCOE is a key parameter used to estimate the economic feasibility of a project [45]. Currently, there is no international standardized approach for producing LCOE. However, the lack of rules and guidance regarding the boundaries and assumptions make LCOE results incomparable and opaque. Generally, three methods are formulated to describe the LCOE: per unit cost of project capacity, sea space utilization area, and power produced. In this paper, LCOE was considered as per unit cost of generating electricity (unit: USD/kWh). It is defined as the sum of all capital costs and lifetime operation and maintenance costs divided by the electricity generation provided to the grid accumulated throughout the lifetime of the technology. By defining sets of parameters such as capital expenditures (CAPEX), installation expenditures (INEX), operational and maintenance expenditures (OPEX), and output energy, a clear and unbiased model is formulated to calculate the LCOE of a tidal current farm project.

Previous related research [1,45] had shown that the cost of a tidal current farm project is primarily composed of CAPEX, INEX and OPEX. The longer the offshore distance is, the higher the values of INEX and OPEX are. In this paper, three assumptions were proposed because no accurate cost modelling about CAPEX, INEX and OPEX have been conducted yet. Firstly, the overall cost (OAC) gradually reduces with an increase in the installed turbines in accordance with Equation (7), as shown in Figure 5a:

$$OAC(Nt) = (2.08 + 1.41 \times e^{-0.0007 \times Nt^2}) \times 10^6 \tag{7}$$

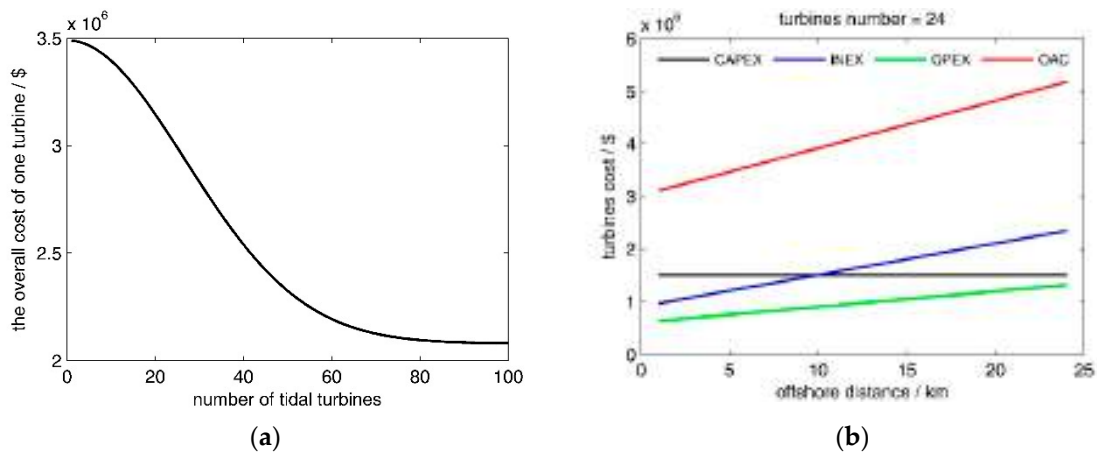


Figure 5. (a) Footprint of the overall cost of one turbine with respect to the number of turbines, and (b) cost of a tidal farm with respect to the number of turbines.

Secondly, CAPEX is a constant value for one tidal turbine, whereas INEX and OPEX both increase at a rate of USD 60,000/km when the offshore distance is >5 km. Thirdly, for one tidal turbine, the ratio of CAPEX:INEX:OPEX is set at 5:4:1. The cost of a tidal current farm with respect to the number of turbines is illustrated in Figure 5b.

In Equation (7), Nt represents the number of turbines in a tidal current project. If $Nt = 24$, then $OAC(Nt) = \text{USD } 3.02 \text{ million}$. Therefore, the cost model for the entire tidal project is expressed as follows:

$$OAC_{project} = \sum_{i=1}^{Nt} (CAPEX_i + INEX_i + OPEX_i) \tag{8}$$

$$CAPEX_i = 3.02 \times 10^6 \times 50\%$$

$$INEX_i = 3.02 \times 10^6 \times 40\% + 60000 \times (s_i - 5)$$

$$OPEX_i = 3.02 \times 10^6 \times 10\% + 60000 \times (s_i - 5)$$

where s_i represents the offshore distance (km). The effective cost of the project per unit power generation is defined as

$$LCOE = \frac{OAC_{project}}{Power\ Produced_{project}} \tag{9}$$

2.7. Objective Function

The incident velocity at each turbine depends on its relative location. Assuming the velocity at turbine i is $u_i(z_i, t)$ ($i = 1, 2, \dots, Nt$), the power generation $P(u_i(z_i, t))$ can be described as follows

$$P = \frac{1}{2} \rho \cdot u_i^3 \cdot \eta_{total} \cdot S \tag{10}$$

The total generated energy by Nt turbines during the period of T hours is

$$E(Z) = \sum_{i=1}^{Nt} \int_0^T P[u_i(z_i, t)] dt \tag{11}$$

where $E(Z)$ is the total generating capacity; ρ is the density of sea water ($=1023 \text{ kg/m}^3$); η is the total conversion efficiency of a turbine, which is calculated by comparing the amount of actual energy production during a given period with the theoretical capacity if it were possible for the turbine to operate at full rated power over this same period; S is the swept area of rotor blade (m^2). The objective function LCOE is obtained using

$$LCOE = \frac{OAC_{project}}{\sum_{i=1}^{Nt} \int_0^T P[u_i(z_i, t)] dt} \tag{12}$$

Therefore, the purpose of this paper is to resolve the optimal layout, in which the per unit cost of power produced is minimized.

3. The QDPS Algorithm

3.1. The Quantum Discrete Particle Swarm (QDPS) Algorithm

The standard particle swarm algorithm is a parallel population-based computation technique proposed by Kennedy and Eberhart [46], which was motivated by the behavior of organisms such as shoaling fish and flocking birds. The standard particle swarm algorithm was originally proposed for continuous optimization problems. In such research, discrete data are used to process the target problems. Therefore, a discrete particle swarm algorithm is befitting realization of discrete optimization problems. In this study, we adopted the quantum discrete particle swarm (QDPS) algorithm proposed by Yang et al. [47]. A quantum particle's position and vector can be defined as follows:

$$Z = [Z_1, Z_2, \dots, Z_M], Z_i = [z_i^1, z_i^2, \dots, z_i^N] \tag{13}$$

where M is the swarm size, N is the particle length (also, the number of tidal turbines), and $z_i^j \in \{0, 1\}$ represents the corresponding discrete particle position of the quantum particle ($i = 1, 2, \dots, M; j = 1, 2, \dots, N$). The algorithm can be expressed as follows:

$$v_{pbest,i}^k = \alpha \cdot z_{pbest,i}^k + \beta (1 - z_{pbest,i}^k) \tag{14}$$

$$v_{gbest}^k = \alpha \cdot z_{gbest}^k + \beta (1 - z_{gbest}^k) \tag{15}$$

$$v_i^{k+1} = \omega v_i^k + c_1 v_{pbest,i}^k + c_2 v_{gbest}^k \tag{16}$$

For each z_i^j ($i = 1, 2, \dots, M; j = 1, 2, \dots, N$), a random number is generated in the range $[0,1]$. If the random number is greater than v_i^j , then $z_i^j = 1$; otherwise, $z_i^j = 0$. The position is then updated as

$$z_i^{k+1} = \begin{cases} 1, & rand() > v_i^{k+1} \\ 0, & rand() \leq v_i^{k+1} \end{cases} \tag{17}$$

where $0 \leq rand() \leq 1; \alpha + \beta = 1, 0 < \alpha, \beta < 1$, which are the control parameters that indicate the degree of control of v_i^d ; ω, c_1 , and c_2 are the coefficients of inertial weight, cognitive, and society study, respectively, where $0 < \omega, c_1, c_2 < 1$, and $\omega + c_1 + c_2 = 1$.

3.2. The Improved Algorithm

First, the simulating domain is discrete into a matrix of $p \times k$ dimensions. We can initialize M matrices by representing the number of quantum particles; each matrix is composed of values of 0 or 1. If the value is 1, the position of the discrete point represents a turbine. Then, each matrix of $p \times k$ dimensions convert into $(p \times k) \times 1$ dimensions, which is the original position of the quantum particle. The objective function is solved according to the generated energy equation and each turbine array, with the results being sorted in a descending order. Finally, the TCTA is optimized through the QDPS algorithm with both updated position and velocity. To ensure the universality of the updated position, the equation of the velocity updated in the QDPS algorithm is described as follows:

$$v_k(t + 1) = \begin{cases} F(x_k(t)), & rand() > p \\ T(x_k(t)), & rand() < p \end{cases} \tag{18}$$

where v is a matrix of $(p \times k) \times 1$ dimensions, which consists of values of 0, -1 , and 1. The initial values of v are 0. $F(x)$ and $T(x)$ are random selection functions. When the particle selects $F(x)$ by probability p , the updated velocity v is replaced by -1 at the position where the generated energy is minimum among the points of $x = 1$. For any one position where $x = 0$, the updated velocity v is replaced by 1, while the value at the other positions remains 0. Therefore, $v_k(t + 1)$ is obtained, $\sum_{i=1}^{p \cdot k} v_i = 0$, and $\sum_{i=1}^{p \cdot k} |v_i| = 2$. When the particle selects $T(x)$ by probability $1 - p$, the update velocity v is replaced by -1 for any two positions where $x = 1$. For any two positions where $x = 0$, the update velocity v is replaced by 1, while the value at the other positions remains 0. Therefore, $v_k(t + 1)$ is obtained, $\sum_{i=1}^{p \cdot k} v_i = 0$, and $\sum_{i=1}^{p \cdot k} |v_i| = 4$.

Thus, the equation of position update can be expressed as follows:

$$x_k(t + 1) = x_k(t) + v_k(t + 1) \tag{19}$$

If the generated energy at the next iteration is greater than at the previous iteration, the array of the next iteration will replace the array of the previous iteration. Then, the algorithm continues to iterate until the optimal population is obtained or the set number of iterations is performed. The process of implementing the QDPS algorithm is described as follows:

- Step 1: Initialize the quantum particles Z and the discrete particles X ;
- Step 2: For discrete particles X , calculate the objective function;
- Step 3: Calculate the optimal position of each particle $Z_{localbest}$;
- Step 4: Calculate the optimal position among all particles in the swarm $Z_{globalbest}$;
- Step 5: Calculate the update velocity of each particle;
- Step 6: Calculate the discrete particles X ;
- Step 7: Loop to Step 2 until one of the stopping criteria (generally, a sufficiently satisfactory object or a specified number of iterations) is satisfied.

4. Illustration

4.1. Computational Domain

According to previous research, it is known that the tidal energy resource around the *Zhoushan* Islands is rich [48,49]. Therefore, this paper used an unstructured-grid coastal ocean model with a resolution refinement for the region of the *Putuo–Hulu* waterway in the *Zhoushan* Islands. The model covered the entire *Hangzhou* Bay, with grid size ranging from approximately 2 km along the open boundary to 20 m around the potential TCTA site. Open boundary conditions for the model were specified at the eastern side of *Hangzhou* Bay using nine harmonic tidal constituents (including S_2 , M_2 , N_2 , K_2 , K_1 , P_1 , O_1 , Q_1 , and M_4) provided via the global tidal model TPX09. The model mesh and bathymetry are shown in Figure 6.

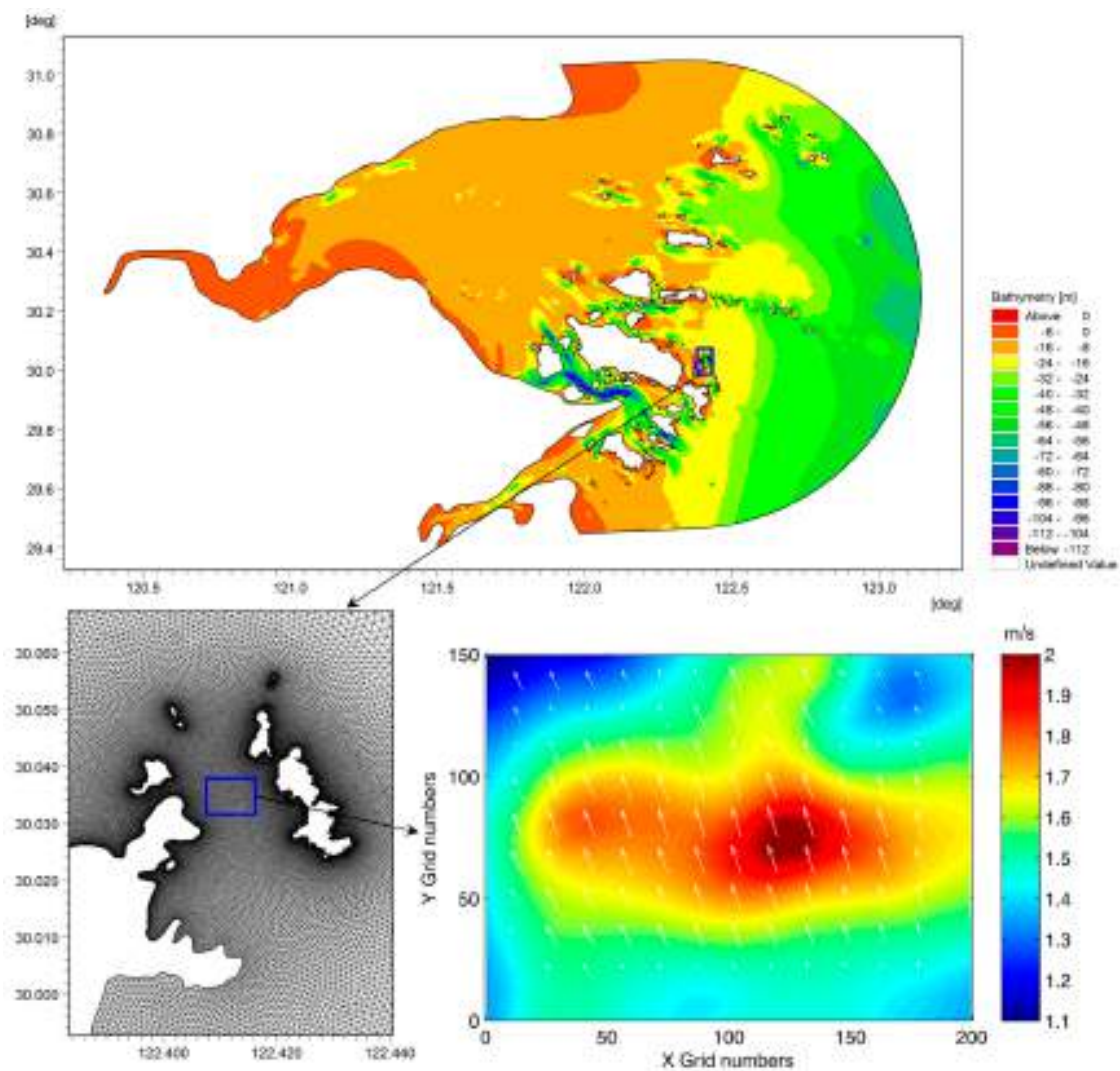


Figure 6. Model domain and bathymetry covering the *Putuo–Hulu* waterway.

The model was validated using field observation data from one tide gauging station and two tidal current stations. The model results and field measurements showed good numerical agreement with an average error in water levels and velocities of 0.05 m and 0.1 m/s, respectively [49].

The QDPS algorithm has been verified using flood and ebb tide current data from the north of the *Putuo–Hulu* waterway. The computing limit is $600 \times 800 \text{ m}^2$, and the averaged depth is 31.1 m. The computational domain is discretized to a $4 \times 4 \text{ m}^2$ structured grid. The bathymetric map and the tidal current rose diagram in the optimized discrete domain are illustrated in Figure 7a,b, respectively. The maximum and minimum values of current

speed in the flood tide are 2.03 m/s and 1.09 m/s, respectively. The averaged current phase is 338.6° . The maximum and minimum current speed in the ebb tide are 1.96 m/s and 1.20 m/s, respectively, and the averaged current direction is 159.1° . It is shown that the tidal current is a typical alternating current along the southeast (SE) and northwest (NW) directions. The current speed fields at the flood and ebb tides are shown in Figure 7c,d, respectively. Statistical data regarding the current and depth in the computational domain are presented in Table 1.

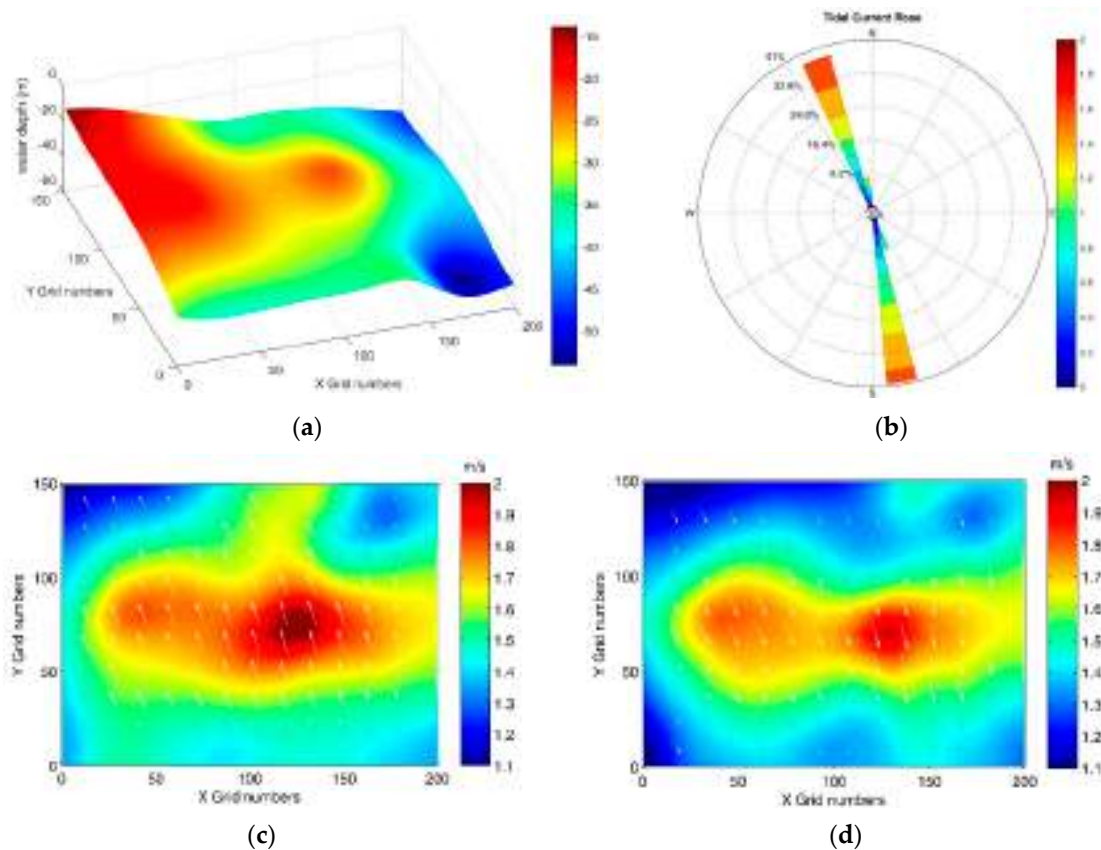


Figure 7. (a) Bathymetric map, (b) tidal current rose diagram of one point, (c) distribution of current speed in the flood tide, and (d) distribution of current speed in the ebb tide (the white arrows represent the current direction).

Table 1. Statistical data regarding current and depth in the computational domain.

Parameters	Current Speed (m/s)		Current Direction ($^\circ$)		Depth (m)	
	Maximum	Minimum	Maximum	Minimum	Maximum	Minimum
Tidal Moment						
Flood tide	2.03	1.09	346.45	325.52	54.0	13.8
Ebb tide	1.96	1.02	168.18	147.01		

4.2. Conformance Testing

The QDPS algorithm was run three times for the flood tide. In this test, the safe distance of $5D$ was chosen, and the other parameters were kept the same as in Section 4.2. The three iterative curves and the optimized layout of the turbines during the flood tide are shown in Figure 8a,b, respectively. The maximum generated energy converges to a stable state, although the rate of iterations varies. The greatest rate of rise was obtained from Step 1 to Step 30, where the generated energy improved by 24%. Thereafter, the rate of growth of generated energy slowed, dropping from 3% during the period of 30–300 steps to only 1% over 300–1500 steps. It can be seen from Figure 8b that most of the turbines

were concentrated within the green areas. According to statistical analysis, the average distance between any two turbines within the green areas was less than $3D$, confirming the consistency among the three layouts.

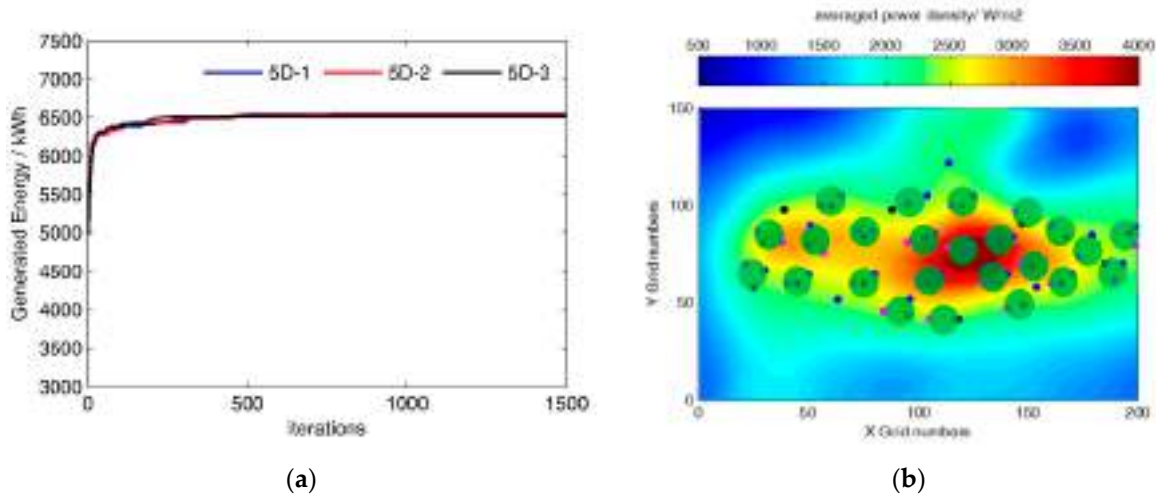


Figure 8. (a) The three iterative curves of optimization in the flood tide, and (b) the three optimized layouts of the turbines in the flood tide (black, blue, and pink points represent the turbines; the bigger green area represents the concentrated coverage of the turbines).

One reason for the different layouts of the turbines is that the layout obtained after 1500 iterations might not be optimal; therefore, a higher number of iterations must be set. Another reason is that there might be more than one optimal layout.

4.3. Safe Distance

The QDPS algorithm was run with three different safe distances, in $3D$, $4D$, and $5D$, respectively, in the ebb tide. The three iterative curves and the optimized layout of the turbines are shown in Figure 9a,b, respectively. The greater the safe distance is, the less extractable energy there is. The layout of the turbines becomes sparser, which is consistent with the power density. The total wake loss at $3D$, $4D$, and $5D$ was 7.2%, 4.1%, and 1.8%, respectively, as the wake loss decreases with increasing safe distance.

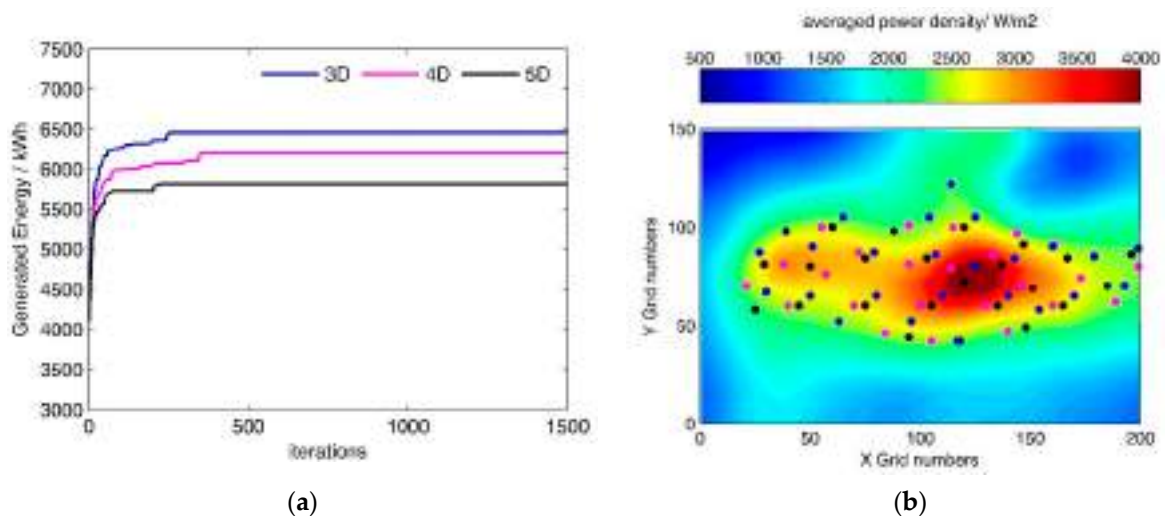


Figure 9. (a) The three iterative curves ($3D$, $4D$, and $5D$) of optimization in the ebb tide, and (b) the three optimized layouts ($3D$, $4D$, and $5D$) of the turbines in the ebb tide (blue, pink and black, points represent turbines of $3D$, $4D$, and $5D$).

5. Results and Discussion

The turbines employed for the tidal farm optimization were SeaGen tidal turbines from Marine Current Turbines (MCT) Ltd. in Bristol of England, which are two-bladed turbines with a rotor diameter of 18 m, and the power curve of turbine is shown in Figure 10a. The characteristics of the ocean terrain and tidal current are as shown in Section 4. The initial tidal farm layout comprised 35 tidal turbines in a 5×7 equidistant ($5D \times 5D$) staggered array, as shown in Figure 10b. The optimization framework was coupled with the QDPS algorithm and Jensen’s wake model to perform tidal farm layout optimization. The parameters used for the QDPS algorithm were swarm size = 15 and the maximum number of iterations = 1000, $\alpha = 0.35$, $\beta = 0.65$, $\omega = 0.1$, $c_1 = 0.4$, and $c_2 = 0.5$.

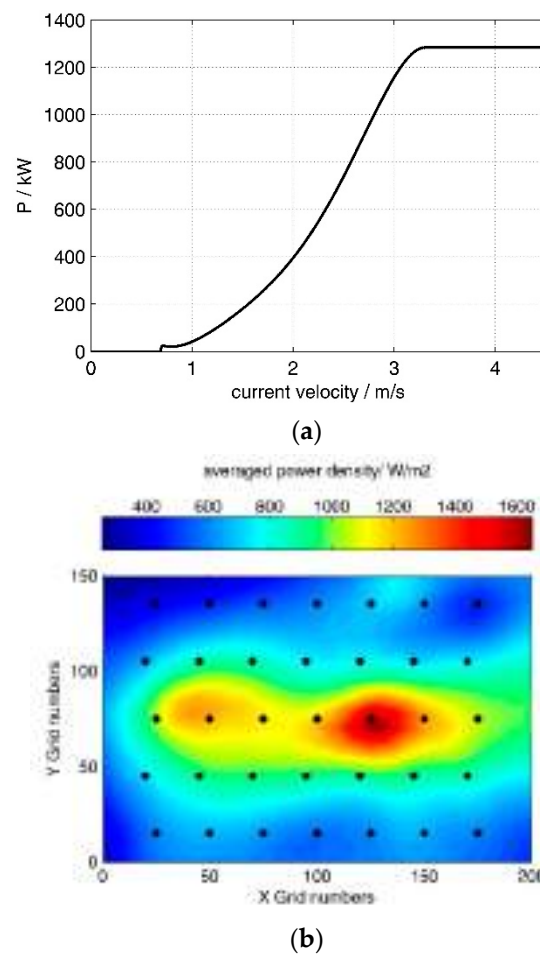


Figure 10. (a) Power curve of tidal turbine, and (b) the initial layout of the tidal turbine array (black points represent turbines).

The optimization was performed for two cases. In Case 1, the cost of the tidal farm was not considered, and the optimization was performed solely to maximize the annual generated energy E (Equation (11)). In this Case 1, the E of the tidal farm at a particular location was calculated by multiplying the averaged power density by the operating time. On the other hand, in Case 2, the cost of the tidal farm was considered, and optimization was performed to minimize the LCOE (Equation (12)).

The optimization was performed three times. For the two cases, the performance of the tidal farm is shown in Table 2. The results show that power production is improved, and the LCOE is reduced when the turbine arrayment is optimized. Therefore, autonomous intelligent optimization can be achieved using the QDPS algorithm, and the optimal velocity is rapid. The iterative curves for both cases are shown in Figure 11a,b, respectively. Both cases predict similar trends of power generation and LCOE. The optimized layouts for

Case 1 and Case 2 resulted in an increase in annual energy production of 16% and 19%, respectively. Moreover, the tidal farm power increased by 22% and 20% in Case 1 and Case 2, respectively. It can be seen from Figure 10a that annual energy production gradually rises with the objective function, while LCOE fluctuated within the range of 3.75–3.91 USD/kWh in Case 1. However, an opposite trend of change is observed in Case 2, where the objective function of LCOE increased continually when the annual energy production reciprocated with a rise from 24,376 MWh to 25,595 MWh. LCOE reduced by 15% in Case 2, which is 3% more than in Case 1, due to the different optimal objective function. The results revealed that greater energy production and lower LCOE could be obtained when LCOE was adopted as the objective function; however, they may not obtain the most optimal value at the same layout of tidal turbine arrays. This is due to the factors impacting the objective function having a different weight. When the maximum energy production is obtained in one layout, LCOE may not obtain the minimum value. In addition, the overall costs in Case 2 reduced by USD 5 million compared to Case 1. Therefore, LCOE is more valuable in tidal farm engineering.

Table 2. Performance of optimized tidal farms and percent changes from reference farm (in brackets).

	Reference on Initial Layout	Case 1	Case 2
Energy production (in MWh)	21,552	25,697 (19%)	≈24,922 (16%)
Farm power (in MW)	6.84	8.62 (22%)	8.24 (20%)
Sea space utilization (in km ²)	0.40	0.31 (−22%)	0.30 (−24%)
LCOE (in USD/kWh)	4.43	≈3.81 (−12%)	3.73 (−15%)

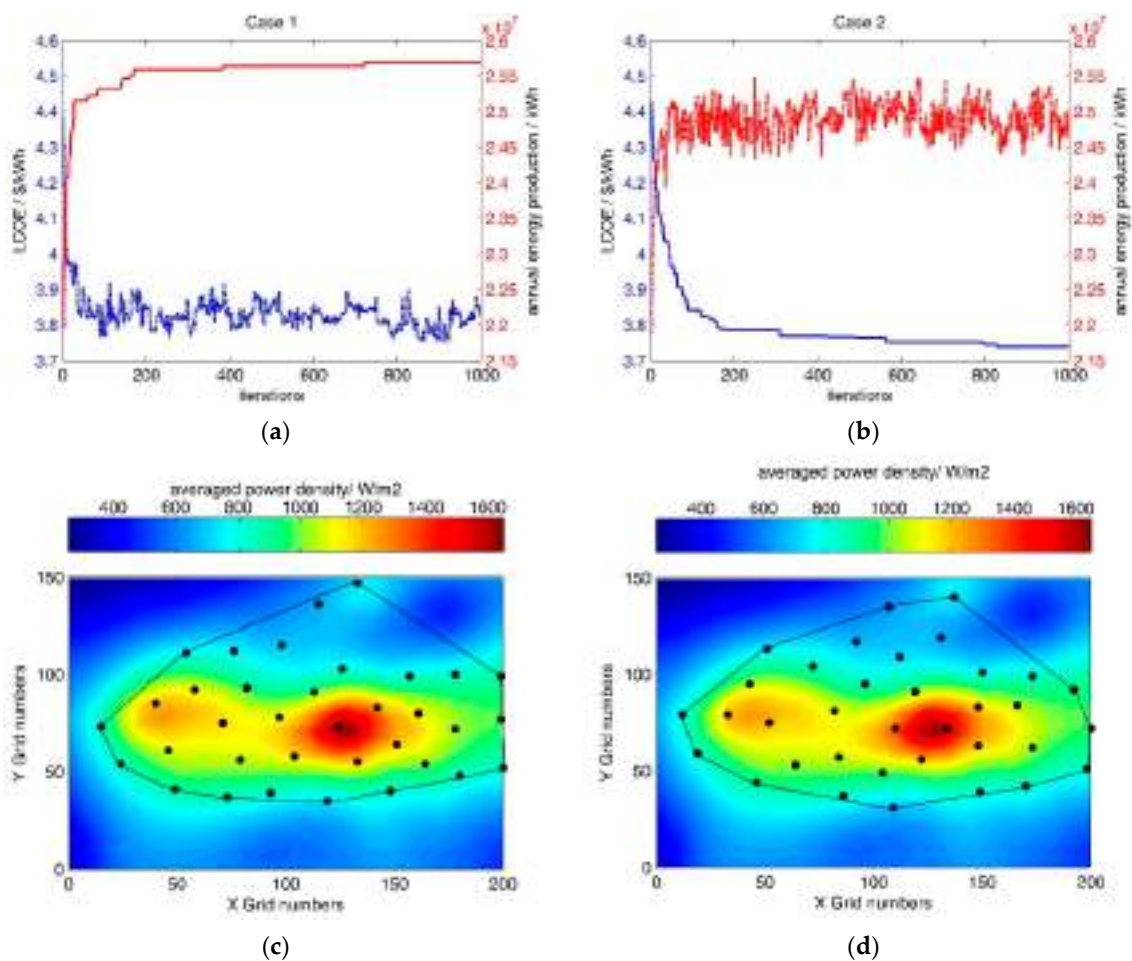


Figure 11. Iterative curve and optimized layout: (a,c) Case 1, and (b,d) Case 2 (black points represent turbines).

The optimized TCTA layout is shown in Figure 11c,d. It can be seen that the optimizing measure attempts to decrease the distance between the turbines and increase the power density at the turbine locations. Therefore, both optimized layouts feature smaller sea space utilization. This again indicates that the optimization problem can be effectively resolved using a multi-constraint multi-objective framework.

6. Conclusions

This paper proposed a method for optimizing the layout of a TCTA using the QDPS algorithm, which is based on the standard particle swarm and Jensen's wake model. The method takes into account different tidal current distributions caused by different TCTA layouts and uses maximum energy production and minimum LCOE as objective function in the QDPS algorithm. The input parameters include tidal current speed, turbine diameter, and constraint conditions such as safe operating distance and water depth. The optimization method based on the QDPS algorithm was applied and verified with flood and ebb tidal current data from the Putuo–Hulu waterway in Zhoushan Islands, China. The results demonstrate that autonomous intelligent optimization can be achieved through the QDPS algorithm. Compared to a traditional staggered layout, the total power generation increases by 19% (Case 1) 16% (Case 2), while the LCOE decreases by 12% (Case 1) 15% (Case 2) when optimization was performed to maximize the annual generated energy (Case 1) and minimize the LCOE (Case 2), respectively. Note that Case 1 and Case 2 may not obtain the most optimal layout at the same time because the factors have different affect weight. The framework based on the QDPS algorithm can be used as a scientific tool for micro-siting a tidal farm and for the preliminary assessment of a tidal current energy resource. In the future works, several main extensions would be required for the application of this method in an industrial setting. Interactions between the bathymetry and turbine wakes should be considered for better optimization of the turbine farm layout. Turbines with different diameters, rated power, and cost should be incorporated into the framework.

Author Contributions: Conceptualization, H.W. and Y.W.; methodology, H.W. and Y.W.; software, Y.W.; validation, H.W. and Y.W.; formal analysis, H.W.; investigation, H.W. and resources, H.W.; data curation, Y.W.; writing—original draft preparation, Y.W. and H.W.; writing—review and editing, H.W., H.-S.K. and H.L.; visualization, Y.W. and H.L.; supervision, H.-S.K.; project administration, H.W.; funding acquisition, H.W. All authors have read and agreed to the published version of the manuscript.

Funding: This research was funded by the National Natural Science Foundation of China, Grant No 42276228.

Institutional Review Board Statement: Not applicable.

Informed Consent Statement: Not applicable.

Data Availability Statement: The data presented in this study are available from the corresponding author upon reasonable request.

Acknowledgments: The authors are grateful to the editors and anonymous reviewers for their constructive comments.

Conflicts of Interest: The authors declare no conflict of interest.

References

1. Fraenkel, P.L. Tidal current energy technologies. *Ibis* **2006**, *148*, 145–151. [[CrossRef](#)]
2. Bahaj, A.S. Generating electricity from the oceans. *Renew. Sustain. Energy Rev.* **2011**, *15*, 3399–3416. [[CrossRef](#)]
3. Myers, L.E.; Bahaj, A.S. An experimental investigation simulating flow effects in first generation marine current energy converter arrays. *Renew. Energy* **2012**, *37*, 28–36. [[CrossRef](#)]
4. Simon, H.; Anna, D.; Fraser, J. *Meygen-Subsea Hub Decommissioning Programme*; MeyGen Ltd.: Edinburgh, UK, 2020.
5. Wu, Y.N.; Wu, G.W.; Wu, H. Islands Marine Renewable Energy Application Requirement and Discussion on Developing Proposal. *Ocean Dev. Manag.* **2017**, *34*, 39–44.

6. Ammara, I.; Leclerc, C.; Masson, C. A viscous three-dimensional differential/actuator-disk method for the aerodynamic analysis of wind farms. *J. Sol. Energy Eng. Trans. ASME* **2002**, *124*, 345–356. [[CrossRef](#)]
7. Myers, L.; Bahaj, A.S. Simulated electrical power potential harnessed by marine current turbine arrays in the Alderney Race. *Renew. Energy* **2005**, *30*, 1713–1731. [[CrossRef](#)]
8. Garrett, C.; Cummins, P. Generating Power from Tidal Currents. *J. Waterw. Port Coast. Ocean Eng.* **2004**, *130*, 114–118. [[CrossRef](#)]
9. Garrett, C.; Cummins, P. Limits to tidal current power. *Renew. Energy* **2008**, *33*, 2485–2490. [[CrossRef](#)]
10. Baker, N.F.; Stanley, A.P.J.; Thomas, J.J.; Ning, A.; Dykes, K. Best practices for wake model and optimization algorithm selection in wind farm layout optimization. In Proceedings of the AIAA Scitech 2019 Forum, San Diego, CA, USA, 7–11 January 2019. [[CrossRef](#)]
11. MacLeod, A.J.; Barnes, S.; Rados, K.G.; Bryden, I.G. Wake effects in tidal current turbine farms. In Proceedings of the MAREC Conference, Newcastle, UK, 1 January 2002; pp. 49–53.
12. Lo Brutto, O.A.; Guillou, S.S.; Thiébot, J.; Gualous, H. Assessing the effectiveness of a global optimum strategy within a tidal farm for power maximization. *Appl. Energy* **2017**, *204*, 653–666. [[CrossRef](#)]
13. Myers, L.E. Operational Parameter of Horizontal Axis Marine Current Turbines. Ph.D. Thesis, University of Southampton, Southampton, UK, 2005.
14. Mycek, P.; Gaurier, B.; Germain, G.; Pinon, G.; Rivoalen, E. Experimental study of the turbulence intensity effects on marine current turbines behaviour. Part I: One single turbine. *Renew. Energy* **2014**, *66*, 729–746. [[CrossRef](#)]
15. Mycek, P.; Gaurier, B.; Germain, G.; Pinon, G.; Rivoalen, E. Experimental study of the turbulence intensity effects on marine current turbines behaviour. Part II: Two interacting turbines. *Renew. Energy* **2014**, *68*, 876–892. [[CrossRef](#)]
16. Stallard, T.; Feng, T.; Stansby, P.K. Experimental study of the mean wake of a tidal stream rotor in a shallow turbulent flow. *J. Fluids Struct.* **2015**, *54*, 235–246. [[CrossRef](#)]
17. Nash, S.; Olbert, A.I.; Hartnett, M. Towards a low-cost modelling system for optimising the layout of tidal turbine arrays. *Energies* **2015**, *8*, 13521–13539. [[CrossRef](#)]
18. Lee, S.H.; Lee, S.H.; Jang, K.; Lee, J.; Hur, N. A numerical study for the optimal arrangement of ocean current turbine generators in the ocean current power parks. *Curr. Appl. Phys.* **2010**, *10*, S137–S141. [[CrossRef](#)]
19. Divett, T.; Vennell, R.; Stevens, C. Optimization of multiple turbine arrays in a channel with tidally reversing flow by numerical modelling with adaptive mesh. *Philos. Trans. R. Soc. A Math. Phys. Eng. Sci.* **2013**, *371*, 20120251. [[CrossRef](#)]
20. Chen, L.; Wang, H.; Chin, R.J.; Luo, H.; Yao, Y.; Wu, Z. An effective framework for wake predictions of tidal-current turbines. *Ocean Eng.* **2021**, *235*, 109403. [[CrossRef](#)]
21. Roc, T.; Conley, D.C.; Greaves, D. Methodology for tidal turbine representation in ocean circulation model. *Renew. Energy* **2013**, *51*, 448–464. [[CrossRef](#)]
22. Roc, T.; Greaves, D.; Thyng, K.M.; Conley, D.C. Tidal turbine representation in an ocean circulation model: Towards realistic applications. *Ocean Eng.* **2014**, *78*, 95–111. [[CrossRef](#)]
23. Gebreslassie, M.G.; Tabor, G.R.; Belmont, M.R. Investigation of the performance of a staggered configuration of tidal turbines using CFD. *Renew. Energy* **2015**, *80*, 690–698. [[CrossRef](#)]
24. Malki, R.; Masters, I.; Williams, A.J.; Croft, T.N. Planning tidal stream turbine array layouts using a coupled blade element momentum—Computational fluid dynamics model. *Renew. Energy* **2014**, *63*, 46–54. [[CrossRef](#)]
25. Stansby, P.; Stallard, T. Fast optimisation of tidal stream turbine positions for power generation in small arrays with low blockage based on superposition of self-similar far-wake velocity deficit profiles. *Renew. Energy* **2016**, *92*, 366–375. [[CrossRef](#)]
26. Funke, S.W.; Farrell, P.E.; Piggott, M.D. Tidal turbine array optimisation using the adjoint approach. *Renew. Energy* **2014**, *63*, 658–673. [[CrossRef](#)]
27. Vennell, R.; Funke, S.W.; Draper, S.; Stevens, C.; Divett, T. Designing large arrays of tidal turbines: A synthesis and review. *Renew. Sustain. Energy Rev.* **2015**, *41*, 454–472. [[CrossRef](#)]
28. Grady, S.A.; Hussaini, M.Y.; Abdullah, M.M. Placement of wind turbines using genetic algorithms. *Renew. Energy* **2005**, *30*, 259–270. [[CrossRef](#)]
29. Zhang, C.; Zhang, J.; Tong, L.; Guo, Y.; Zhang, P. Investigation of array layout of tidal stream turbines on energy extraction efficiency. *Ocean Eng.* **2020**, *196*, 106775. [[CrossRef](#)]
30. Wan, C.Q.; Wang, J.; Yang, G. Optimal Micro-siting of Wind Farm Based on Weibull Distributon. *Acta Energiæ Sol. Sin.* **2011**, *32*, 999–1004.
31. Abdelsalam, A.M.; El-Shorbagy, M.A. Optimization of wind turbines siting in a wind farm using genetic algorithm based local search. *Renew. Energy* **2018**, *123*, 748–755. [[CrossRef](#)]
32. Pookpant, S.; Ongsakul, W. Optimal placement of wind turbines within wind farm using binary particle swarm optimization with time-varying acceleration coefficients. *Renew. Energy* **2013**, *55*, 266–276. [[CrossRef](#)]
33. Wang, C.J.; Wang, X.H.; Chen, G.C. Tidal Current Turbines Micrositing Based on Improved Differential Evolution Algorithm. *Trans. China Electrotech. Soc.* **2016**, *31*, 99–108.
34. Liu, C.; Wang, K.; Wang, X.H. Optimal deployment of tidal current turbines based on particle swarm algorithm. *J. Zhejiang Univ. (Eng. Sci.)* **2013**, *47*, 2088–2093.
35. Wu, G.W.; Wu, H.; Wang, X.Y.; Zhou, Q.W.; Liu, X.M. Tidal Turbine Array Optimization Based on the Discrete Particle Swarm Algorithm. *China Ocean Eng.* **2018**, *32*, 358–364. [[CrossRef](#)]

36. Lo Brutto, O.A.; Nguyen, V.T.; Guillou, S.S.; Thiébot, J.; Gualous, H. Tidal farm analysis using an analytical model for the flow velocity prediction in the wake of a tidal turbine with small diameter to depth ratio. *Renew. Energy* **2016**, *99*, 347–359. [[CrossRef](#)]
37. Lo Brutto, O.A.; Thiébot, J.; Guillou, S.S.; Gualous, H. A semi-analytic method to optimize tidal farm layouts—Application to the Alderney Race (Raz Blanchard), France. *Appl. Energy* **2016**, *183*, 1168–1180. [[CrossRef](#)]
38. Chen, C.; Beardsley, R.C.; Cowles, G. *An Unstructured Grid, Finite-Volume Coastal Ocean Model: FVCOM User Manual*, 2nd ed.; Citeseer: State College, PA, USA, 2006; Volume 19, pp. 78–89.
39. Palm, M.; Huijsmans, R.; Pourquie, M. The application of semi-empirical wake models for tidal farms. In Proceedings of the 9th European Wave and Tidal Energy Conference Series (EWTEC), Southampton, UK, 5–9 September 2011.
40. Wang, S.; Lam, W.H.; Cui, Y.; Zhang, T.; Jiang, J.; Sun, C.; Guo, J.; Ma, Y.; Amill, G. Novel energy coefficient used to predict efflux velocity of tidal current turbine. *Energy* **2018**, *158*, 730–745. [[CrossRef](#)]
41. Wang, S.; Lam, W.H.; Cui, Y.; Zhang, T.; Jiang, J.; Sun, C.; Guo, J.; Ma, Y.; Hamill, G. Semi-empirical wake structure model of rotors using joint axial momentum theory and DES-SA method. *Ocean Eng.* **2019**, *191*, 106525. [[CrossRef](#)]
42. Jensen, N.O. *A Note on Wind Generator Interaction*; RisØ National Laboratory: Roskilde, Denmark, 1983.
43. Graham, R. An efficient algorithm for determining the convex hull of a finite planar set. *Inf. Process. Lett.* **1972**, *1*, 73–82. [[CrossRef](#)]
44. Bourke, P. *Calculating the Area and Centroid of a Polygon*; Swinburne University of Technology: Hawthorn, Australia, 1988.
45. Previsic, M.; Chozas, J. *International Levelised Cost of Energy for Ocean Energy Technologies*; Ocean Energy System: Lisbon, Portugal, 2015.
46. Kennedy, J.; Eberhart, R.C. Particle swarm optimization. In Proceedings of the IEEE International Conference on Neural Networks, Perth, Australia, 27 November–1 December 1995; Volume 4, pp. 1942–1948.
47. Yang, S.; Wang, M.; Jiao, L. A quantum particle swarm optimization. In Proceeding of the 2004 IEEE Congress on Evolutionary Computation, Portland, OR, USA, 19–23 June 2004; Volume 1, pp. 320–324.
48. Hou, F.; Yu, H.M.; Bao, X.W.; Wu, H. Analysis of tidal current energy in Zhoushan sea area based on high resolution numerical modeling. *Sol. Energy* **2014**, *35*, 125–133.
49. Wu, Y.N.; Wu, H.; Feng, Z. Assessment of tidal current energy resource at Putuo Mountain-Hulu Island waterway. *Renew. Energy Resour.* **2017**, *35*, 1566–1573.

Disclaimer/Publisher’s Note: The statements, opinions and data contained in all publications are solely those of the individual author(s) and contributor(s) and not of MDPI and/or the editor(s). MDPI and/or the editor(s) disclaim responsibility for any injury to people or property resulting from any ideas, methods, instructions or products referred to in the content.